Biochimica et Biophysica Acta 1838 (2014) 2205–2215

Contents lists available at ScienceDirect

Biochimica et Biophysica Acta

journal homepage: www.elsevier.com/locate/bbamem

Comparison of reversible membrane destabilisation induced by antimicrobial peptides derived from Australian frogs ☆

Tzong-Hsien Lee [a], Christine Heng [a], Frances Separovic [b], Marie-Isabel Aguilar [a,*]

[a] Department of Biochemistry and Molecular Biology, Monash University, Clayton, VIC 3800, Australia
[b] School of Chemistry, Bio21 Institute, University of Melbourne, Melbourne, VIC 3010, Australia

ARTICLE INFO

Article history:
Received 13 November 2013
Received in revised form 21 January 2014
Accepted 21 February 2014
Available online 1 March 2014

Keywords:
Frog antimicrobial peptides
Citropin
Caerin
Dual polarisation interferometry
Phospholipid membranes

ABSTRACT

The membrane destabilising properties of the antimicrobial peptides (AMP) aurein 1.2, citropin 1.1, maculatin 1.1 and caerin 1.1, have been studied by dual polarisation interferometry (DPI). The overall process of peptide induced membrane destabilisation was examined by the changes in bilayer order as a function of membrane-bound peptide mass per unit area and revealed three different modes of action. Aurein 1.2 was the only peptide that significantly destabilised the neutral membrane (DMPC), while all four peptides induced destabilisation of the negatively charged membrane (DMPC/DMPG). On DMPC, citropin 1.1, maculatin 1.1 and caerin 1.1 bound irreversibly at low concentrations but caused a reversible drop in the bilayer order. In contrast to DMPC/DMPG, these three peptides caused a mass drop at the higher concentrations, which may correspond to insertion and bilayer expansion. The critical level of bound peptide necessary to induce membrane destabilisation (peptide:lipid ratio) was determined and correlated with peptide structure. As the most lytic peptide, aurein 1.2 adsorbed strongly prior to dissolution of the bilayer. In contrast, the binding of citropin 1.1, maculatin 1.1 and caerin 1.1 needed to reach a critical level prior to insertion into the membrane and incremental expansion and disruption. Our results demonstrate that sequential events can be monitored in real-time under fluidic conditions to elucidate the complex molecular mechanism of AMP action. In particular, the analysis of birefringence in real time allows the description of a detailed mechanistic model of the impact of peptides on the membrane bilayer order. This article is part of a Special Issue entitled: Interfacially Active Peptides and Proteins. Guest Editors: William C. Wimley and Kalina Hristova.

1. Introduction

Currently, one of the major challenges facing the medical field is the increase in frequency of resistance to multiple antibiotics [1–3]. The antimicrobial peptides (AMPs) are widely distributed and are excellent candidates for the development of effective therapeutics due to their ability to kill a broad spectrum of bacteria, fungi and cancer cells [4], commonly exerting their effects within minutes as compared to hours for common antibiotics via destabilisation of the cell membrane. However, better understanding of the interplay between AMPs and lipid membranes and their selectivity and mechanism of action is necessary for the design of selective and potent antibacterial peptides.

The skin secretions of many amphibians are rich sources of novel compounds that include highly potent AMPs [5]. In this study, we have investigated the membrane interaction of four peptides isolated from several species of Australian tree frogs, namely aurein 1.2, citropin 1.1, maculatin 1.1 and caerin 1.1. Previous studies have shown that these four peptides exhibit selectivity against G(+) bacteria and are less effective or inactive against G(−) bacteria [6]. The sequence and structural features of these peptides are central to their antimicrobial activity and selectivity. Each of these peptides is cationic with a calculated pI between 9.9 and 10.6. Despite differences in length, aurein 1.2 (13 residues), citropin 1.1 (16 residues), maculatin 1.1 (21 residues) and caerin 1.1 (25 residues), all have high sequence homology in the N- and C-termini. The increase in length for each peptide roughly coincides with the insertion of one helical turn [7]. Based on structural analysis using FTIR, CD and NMR, these peptides are predominantly unstructured in aqueous solution. However, they readily adopt an amphipathic α-helical structure in membrane mimetic environments [7]. This ability to fold into an amphipathic α-helical conformation in the vicinity of a membrane has been recognised as a critical factor in facilitating the initial interaction of the peptide with the lipid bilayer [7–9]. NMR studies of these peptides in the membrane mimetic environments show that the shorter peptides, aurein 1.2 and citropin 1.1, adopt a single continuous α-helix while the longer peptides, maculatin 1.1 and caerin 1.1, comprise two α-helices separated by a flexible hinge region induced by the presence of one and two proline residues, respectively [7]. The kink structure caused by the proline residues is crucial for

☆ This article is part of a Special Issue entitled: Interfacially Active Peptides and Proteins. Guest Editors: William C. Wimley and Kalina Hristova.

* Corresponding author at: Department of Biochemistry and Molecular Biology, Monash University, Wellington Rd., Clayton, VIC 3800, Australia.
E-mail address: Mibel.Aguilar@monash.edu (M.-I. Aguilar).

http://dx.doi.org/10.1016/j.bbamem.2014.02.017
0005-2736/

their activity and may be important for membrane interaction. Based on solid-state NMR and FTIR results together with dye leakage from GUVs, the modes of action of these peptides are closely linked to their helical length [10]. Aurein 1.2 and citropin 1.1 are short peptides, which hinder their ability to fully penetrate the lipid bilayer, and destabilise the membrane via binding to the interfacial region of membrane [7,11]. The longer peptides, maculatin 1.1 and caerin 1.1, may insert and disrupt the membrane through the formation of pores [7,12,13] as a result of their α-helical length allowing the peptide to penetrate and span the lipid bilayer. Characteristics such as sequence, length, secondary structure, overall net charge, hydrophobicity and amphipathicity, are linked to AMP activity which, therefore, make these four peptides a suitable set for comparison of AMP mechanisms of action and their roles in membrane destabilisation.

To date, the exact mode of action of these peptides is debated, with peptide hydrophobicity, hydrophobic moment, and lipid composition and charge of the target cell membrane also proposed to contribute to the peptide ability to perturb the cellular membrane [14]. However, without the information on the role of the lipid bilayer and the structural and dynamic changes of the bilayer during this interaction, our understanding of the mechanism of AMP action may be over-simplified [15]. We have previously studied the membrane binding characteristics of aurein 1.2 and maculatin 1.1 using SPR and DPI [9,12,16,17]. In particular, we demonstrated that both peptides exert a significant effect on the membrane bilayer structure but, in the case of aurein 1.2, the bilayer was irreversibly disrupted [17] while, in the presence of maculatin, the bilayer was able to recover [9,12]. These results demonstrate that understanding changes in the bilayer structure during peptide binding is as important as analysing the peptide structure and membrane affinity. In the present study we have expanded our analysis to investigate the membrane-disrupting properties of citropin 1.1 and caerin 1.1 and allow a comparative analysis of the membrane disruptive properties across the four peptides. We have used model membrane systems to represent both eukaryotic and bacterial membranes. Specifically, zwitterionic phospholipids such as dimyristoylphosphatidylcholine (DMPC) are used to mimic eukaryotic membranes while the anionic dimyristoylphosphatidylglycerol (DMPG) is used to mimic the properties of negatively charged bacterial cell membranes. We deposited stable membranes on a planar silicon oxynitride biosensor chip which were then used to study the changes in membrane structure throughout the process of binding, insertion and membrane lysis by these four frog peptides in real time using DPI technology [18–20]. This technique provides simultaneous quantification of real time changes in the thickness, mass density and birefringence of the membrane. We hypothesise that changes in birefringence as a function of the amount of each peptide bound to the membrane provide unique insight into the mechanism of binding of these four peptides, and that the disruption of the membrane by the four peptides is preceded by substantial membrane structure changes that can be measured by DPI. The aim of this study, therefore, was to examine and compare the changes in the lipid bilayer structure throughout the sequence of events from initial electrostatic binding of the peptide to the final membrane destabilisation induced by aurein 1.2, citropin 1.1, maculatin 1.1 and caerin 1.1.

2. Materials and methods

2.1. Chemicals and reagents

1,2-Dimyristoyl-sn-glycero-3-phosphocholine (DMPC) and 1,2-dimyristoyl-sn-glycero-3-[phosphor-rac-(1-glycerol)] sodium salt (DMPG) were obtained from Avanti Polar Lipids (Alabaster, AL). 4-morpholinepropanesulfonic acid (MOPS), sodium chloride, calcium chloride and sodium dodecylsulfate (SDS) were purchased from Sigma-Aldrich (St. Louis, MI). Chloroform, methanol, and ethanol were all HPLC-grade solvents purchased from Merck (Darmstadt, Germany). Hellmanex II was obtained from Hellma (Müllheim, Germany). Bovine serum albumin (BSA) was purchased from ThermoFisher Scientific, Scoresby, Australia. Water was quartz-distilled and deionised in a Milli-Q system equipped with UV oxidation to remove organic residue (Millipore, Bedford, MA). Aurein 1.2, citropin 1.1, maculatin 1.1 and caerin 1.1 were purchased from Mimotopes (Melbourne, Australia) and the sequences and molecular properties are listed in Table 1. The purity of peptides (~95%) was analysed using a capillary reversed phase C18 column (Zorbax SB 0.5 × 150 mm, 5 μm, 300 Å, Agilent, St. Clara, CA) using an appropriate 0–60% 0.1% trifluoroacetic acid-acetonitrile gradient. These peptides were further confirmed by ESI-ion trap (1100 series, LC/MSD Trap, Agilent). Peptide concentration was determined by amino acid analysis.

2.2. Liposome preparation

2 mM DMPC stock in chloroform and 2 mM DMPG stock in chloroform/methanol (3:1 v/v) were used for the preparation of dried DMPC and DMPC/DMPG (molar ratio 4:1) films. Appropriate volume of lipid stock solutions was used to make the total lipid amount of 0.8 μmol. The solvent was then evaporated under a gentle stream of N_2 gas and further vacuum dried overnight. The dried lipid thin films were hydrated with the running buffer (10 mM MOPS, pH 7.0, 150 mM NaCl) to make a lipid concentration of 1 mM. The liposome solution was then extruded through a 50 nm polycarbonate membrane 21 times using Liposofast extruder (Avestin, Ottawa, Canada). The size distribution of resulting small unilamellar vesicles (SUVs) was characterised by dynamic light scattering with a Malvern Zetasizer 3000 (Malvern Laboratories Ltd., Malvern, UK).

2.3. Dual polarisation interferometry

Dual polarisation interferometry (DPI) is an analytical method for analysing thin films using a dual optical waveguide interferometric technique [18–20]. Alternate dual orthogonal polarisation allows unique combinations of several opto-geometrical properties, including refractive index (RI), density, thickness, mass and birefringence, to be measured in real time for the layer formation of biomolecules. DPI (Analight BIO200, Farfield Group Ltd., Manchester, UK) comprises a dual slab waveguide sensor chip with an upper sensing waveguide and a lower optical reference waveguide illuminated with an alternating polarised laser beam (HeNe, wavelength 632.8 nm). Two orthogonal

Table 1
Characteristics of AMPs from Australian tree frogs used in this study.

Peptide	Sequence																									Mass	No AA	Charge	[H]	[μH]
	1				5					10					15					20					25					
Aurein 1.2	G	L	F	D	I	I	K	K	–	–	–	–	–	–	–	–	–	–	–	–	I	A	E	S	F	1478	13	+1	0.582	0.765
Citropin 1.1	G	L	F	D	V	I	K	K	V	A	S	–	–	–	–	–	–	–	–	V	I	G	G	L	–	1613	16	+2	0.623	0.614
Maculatin 1.1	G	L	F	G	V	L	A	K	V	A	A	–	–	–	–	H	V	V	P	A	I	A	E	H	F	2145	21	+1	0.435	0.435
Caerin 1.1	G	L	L	S	V	L	G	S	V	A	K	H	V	L	P	H	V	V	P	V	I	A	E	H	L	2583	25	+1	0.734	0.321

[H]: Overall hydrophobicity; [μH]: Mean amphipathic moment. The peptides are aligned according to their sequence homology.
Each peptide has a free N-terminus and a C-terminal amide.

polarizations are passed through the sensor chip creating two different waveguide modes, transverse electric (TE) and transverse magnetic (TM).

2.4. Membrane chip preparation

Unmodified silicon oxynitride FB80 AnaChips (Farfield Group, UK) were used for the preparation of membrane chips. A 100 μm thick silicon mask with two slits is clamped on top of the waveguide chip which provides two separate microfluidic channels over the sensing waveguide. The chip surfaces were cleaned on-line by rinsing 3 times each with 10% Hellmanex II, 2% SDS and absolute ethanol at 50 μL/min. Prior to measurement, the waveguide chips were calibrated with respect to their optical properties using an 80:20 w/w ethanol/water mixture at 20 °C. The flow rate of running buffer was controlled using a Harvard Apparatus PHD2000 programmable syringe pump (Holliston, MA). Typical flow rates were 20 μL/min for liposome deposition and 40 μL/min for peptide binding to the supported lipid bilayer (SLB). The AnaLight200 version 2.1.0 software was used for data acquisition and the acquired data were analysed using AnaLight® Explorer proprietary software. Liposome suspensions (0.1 mg/mL) of DMPC and DMPC/DMPG (4:1) were adsorbed in the presence of 1 mM $CaCl_2$ for 10 min at 28 °C. At the end of the liposome injection, the adsorption was immediately followed by injecting 1 mM $CaCl_2$ in a running buffer for 10 min which facilitates the stabilisation of SLB on the solid substrate. The SLB was further equilibrated in a running buffer without Ca^{++} for 20 min before adjusting temperature to 20 °C. The coverage and quality of membrane were checked with 50 μL injection of 50 μg/mL BSA. No BSA binding was observed for a defect-free membrane bilayer fully covered on the planar silicon oxynitride chip.

2.5. Peptide injection

Each frog peptide was prepared at concentrations of 5 μM, 10 μM and 20 μM in 10 mM MOPS, pH 7, 150 mM NaCl. Peptide samples were injected consecutively in order of increasing concentration onto the deposited bilayer at 20 °C. 180 μL of each peptide concentration was injected at a flow rate of 40 μL/min, followed by a running buffer for 30 min prior to injecting the next concentration onto the same bilayer surface. Each peptide concentration measurement was performed on the same lipid bilayer. Each experiment was performed as a duplicate of duplicates and typical sensorgrams are shown in Fig. 2. After the peptide binding to SLB experiment, the waveguide surface was regenerated with 2% SDS, 10% Hellmanex II and ethanol at 28 °C.

2.6. Optical birefringence analysis of dynamic changes in membrane lipid order

Birefringence (optical anisotropy) is a measure of the difference in RI of two orthogonal polarisations. Amongst various types of thin films, phospholipid bilayers show optical birefringence owing to the liquid crystal properties of lipid molecules self-assembled into uni-axial aligned bilayers. The non-random orientation of lipid molecules in membranes creates an anisotropic system with a uniaxial optical axis with two principal refractive indices, n_e which denotes the extra-ordinary RI with the electric vector polarised parallel to the optical axis, and n_o which is defined as the ordinary RI with the electric vector polarised perpendicular to the optical axis. Difference between these two RI for a lipid film is defined as birefringence, Δn_f where $\Delta n_f = n_e - n_o$. Thus, an additional parameter is generated in DPI through the difference between two effective RI, namely n_{TM} and n_{TE}, measured from two orthogonal waveguide modes, TM and TE. The degree of molecular order, S, of the uniaxial lipid bilayer is defined by the ratio of principal polarizabilities of the bilayer to the molecular polarizabilities. This order parameter (S) is proportional to the birefringence values [18]. Thus, the birefringence values represent an averaged measurement of lipid molecular orientation order and the lipid acyl chain order.

The effective birefringence can only be determined by calculation of the two different RI, n_{TM} and n_{TE}, for each waveguide mode by fixing the thickness or RI of the deposited layer with assumed uniform coverage. The difference between the n_{TM} and n_{TE} will be the true effective birefringence of the adsorbed layer. Changes in the thickness, mass and birefringence of the deposited bilayer can be resolved by fixing the refractive index at a predetermined value of 1.47 for DMPC and DMPC/DMPG [17,19].

2.7. Calculation of mass, thickness, and density for an anisotropic layer

To calculate the absorbed mass of a layer from DPI measurements, the de Feijter formula [17], $m = d(n_{iso} - n_{buffer}) / (dn/dc)_{lipid}$, was employed. The average or corresponding isotropic value of the RI is calculated according to $n_{iso} = ((n^2_{TM} + 2n^2_{TE}) / 3)^{1/2}$ and RI of the MOPS buffer used for these experiments was, $n_{buffer} = 1.3349$ (T = 20 °C). The de Feijter formula assumes that dn/dc (rate of change in RI with concentration) remains constant throughout the whole process of the experiment. For the present analysis, $(dn/dc)_{lipid}$ is approximated to be 0.135 cm^3/g while the $(dn/dc)_{peptide}$ is to be 0.182 cm^3/g. All structural parameters of the adlayers are calculated as described by Mashaghi et al. [18]. An average bilayer thickness of 45.2 ± 0.7 Å (n = 16) and a birefringence of 0.0217 ± 0.0006 was obtained for DMPC while an average bilayer thickness of 52.1 ± 4.5 Å and a birefringence of 0.0254 ± 0.0040 was obtained for DMPC/DMPG (4:1) (n = 16).

2.8. Calculation of mean hydrophobicity <H>

The mean hydrophobicity is calculated using $\langle H \rangle = \frac{1}{N}\sum_{n-1}^{N} H_n$ where N is the sequence length, and H_n is the hydrophobicity of the nth amino acid in the sequence according to its octanol/water partition coefficient [21].

2.9. Calculation of the mean amphipathic moment <μH>

The mean amphipathic moment is calculated with $\langle \mu H \rangle = \frac{1}{N}$ $\left\langle \left[\sum_{n-1}^{N} H_n \sin(n\delta)\right]^2 + \left[\sum_{n-1}^{N} H_n \cos(n\delta)\right]^2 \right\rangle^{1/2}$ where N is the sequence length, H_n is the hydrophobicity of the nth amino acid in the sequence, and $n\delta$ is the angle separating side chains along the backbone with $\delta = 100°$ for an α-helix [22]. The length and the direction of the <μH> vector depend on the hydrophobicity and the position of the side chain along the helix axis. Values for each peptide are listed in Table 1.

3. Results

3.1. Characteristics of Australian tree frog peptides

Several characteristics of the frog peptides studied here are crucial to their mechanisms of action. The four AMPs share common sequence and structural features in their N and C termini, which have been linked to their antimicrobial activity. However, as depicted in Table 1, they differ in length, charge, hydrophobicity and amphipathic moment, which can influence their ability to either insert or surface-bind to the membrane prior to lysis. The peptides possess a net positive charge and the mean hydrophobicity, which reflect the intrinsic capability of the peptides to partition from an aqueous to a hydrophobic phase, increases in order with caerin 1.1 > maculatin 1.1 > citropin 1.1 >aurein 1.2. Each of these peptides also exhibits an amphipathic pattern when folded into a helical structure as shown in Fig. 1, which has been

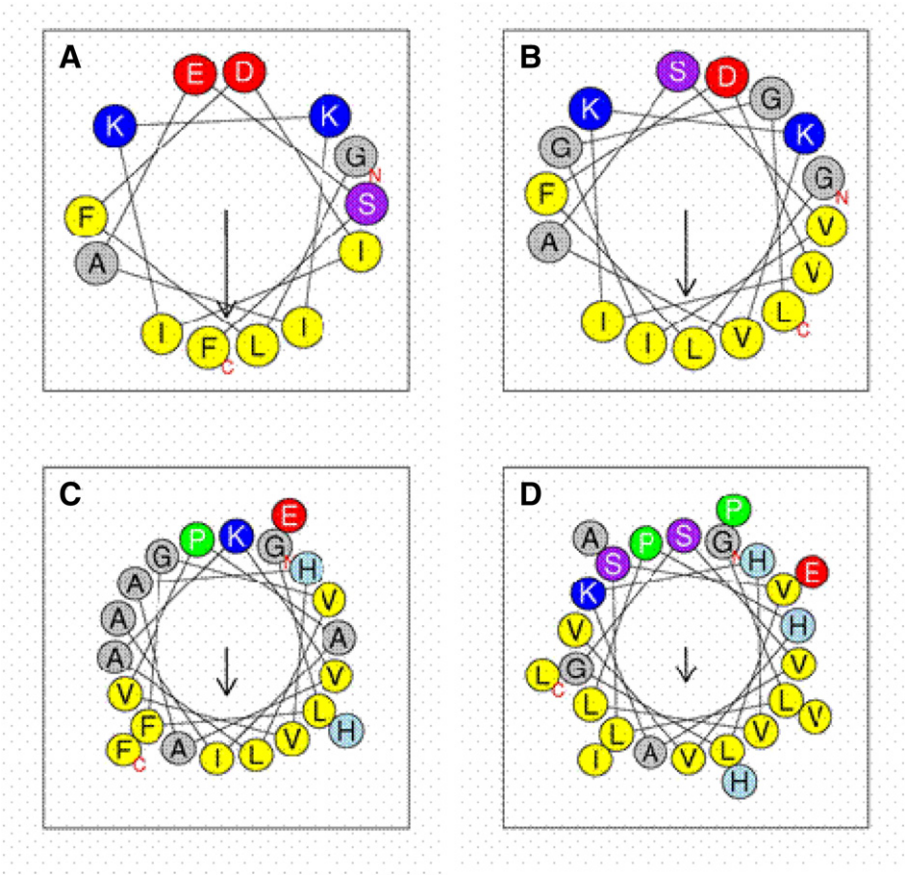

Fig. 1. Helical wheel representation of hydrophobic (yellow) and hydrophilic faces for: (A) aurein 1.2, (B) citropin 1.1, (C) maculatin 1.1, and (D) caerin 1.1, folding into an α-helix. The vector of hydrophobic moment is shown as an arrow from the centre of the helical wheel while the value of the calculated hydrophobic moment is proportional to the length of the arrow. Polar residues (in blue).

recognised as a critical factor in facilitating membrane lysis [7]. Notably, the difference in the calculated amphipathic moments of the peptides, which consists of the vector sum of the hydrophobicities of the individual amino acids, indicates the amphipathic moment of the peptides increases in the order aurein 1.2 > citropin 1.1 > maculatin 1.1 > caerin 1.1. The adoption of significant helical structure in membrane environments by aurein 1.2, maculatin 1.1 and caerin 1.1 has been previously reported [8,13,14] and the corresponding data for citropin 1.1 is shown in Fig. S1 in the Supplementary data.

3.2. Peptide induced changes in DMPC and DMPC/DMPG SLBs

The simultaneous measurement of multiple parameters for membrane bilayers by DPI analysis allows examination of peptide-induced changes in the membrane structure, which can be monitored in real time. The DMPC and DMPC/DMPG bilayers formed at 28 °C were then equilibrated at 20 °C which allow the lateral organisation of the lipid bilayer in the 'gel' phase with a greater degree of lipid orthogonal alignment and higher anisotropic properties. This allows investigation of the structural and dynamic changes occurring within the lipid matrix during AMP interaction, specifically in regard to the analysis of molecular orientation order. For each experiment, consecutive peptide concentrations of 5 μM, 10 μM and 20 μM were injected onto the same SLB, with the higher concentrations similar to the reported minimum inhibitory concentration (MIC) against bacteria [14,23–25]. The accumulative binding of each peptide was first characterised by the TM and TE phase changes as a function of time as shown in Fig. 2A–D for DMPC and Fig. 1H–2E for DPMC/DMPG. The data for aurein 1.2 was published in a previous study [17] and is reproduced here for comparative purposes.

The measured TM and TE phases were subsequently resolved into the mass of membrane-bound peptide and birefringence for both lipid bilayers as previously described [17]. Plots of mass changes versus time and birefringence versus time for each peptide are shown in Fig. 3A–D for DMPC and Fig. 3E–H for DMPC/DMPG. The maximum change in mass in birefringence at the end of the first injection phase was determined to allow a comparison of the relative extent of initial binding of each peptide to a fresh bilayer, and these values are listed in Table 2. For low concentrations of peptide binding to the DMPC layer, all four peptides showed an association and dissociation phase. At the lower concentration (5 μM), the shorter peptides aurein 1.2 and citropin 1.1 bound to the DMPC layer at a slower rate with a maximum mass of 0.31 and 0.278 ng/mm^2 at the end of injection, respectively, and a relatively small increase in mass of 0.17 ng/mm^2 at the end of dissociation (Fig. 3A & B). When 10 μM aurein 1.2 and citropin 1.1 was accumulatively added onto the DMPC layer, the association phase for both peptides was nearly double that observed at 5 μM. However, a similar mass increment was obtained. At 20 μM, a large change was observed during the association of aurein 1.2 to DMPC which, as previously reported, indicates loss of membrane material from the chip surface [17]. Citropin 1.1 exhibited a similar binding profile to aurein 1.2 at 5 μM and 10 μM but there was no significant mass loss at any

Fig. 2 The real time changes in TM and TE for: (A), (B) aurein 1.2; (C), (D) citropin 1.1; (E), (F) maculatin 1.1; and (G), (H) caerin 1.1; binding to a DMPC (A)–(D) or DMPC/DMPG bilayer (E)–(H), at 20 °C at 5 μM, 10 μM and 20 μM peptide.

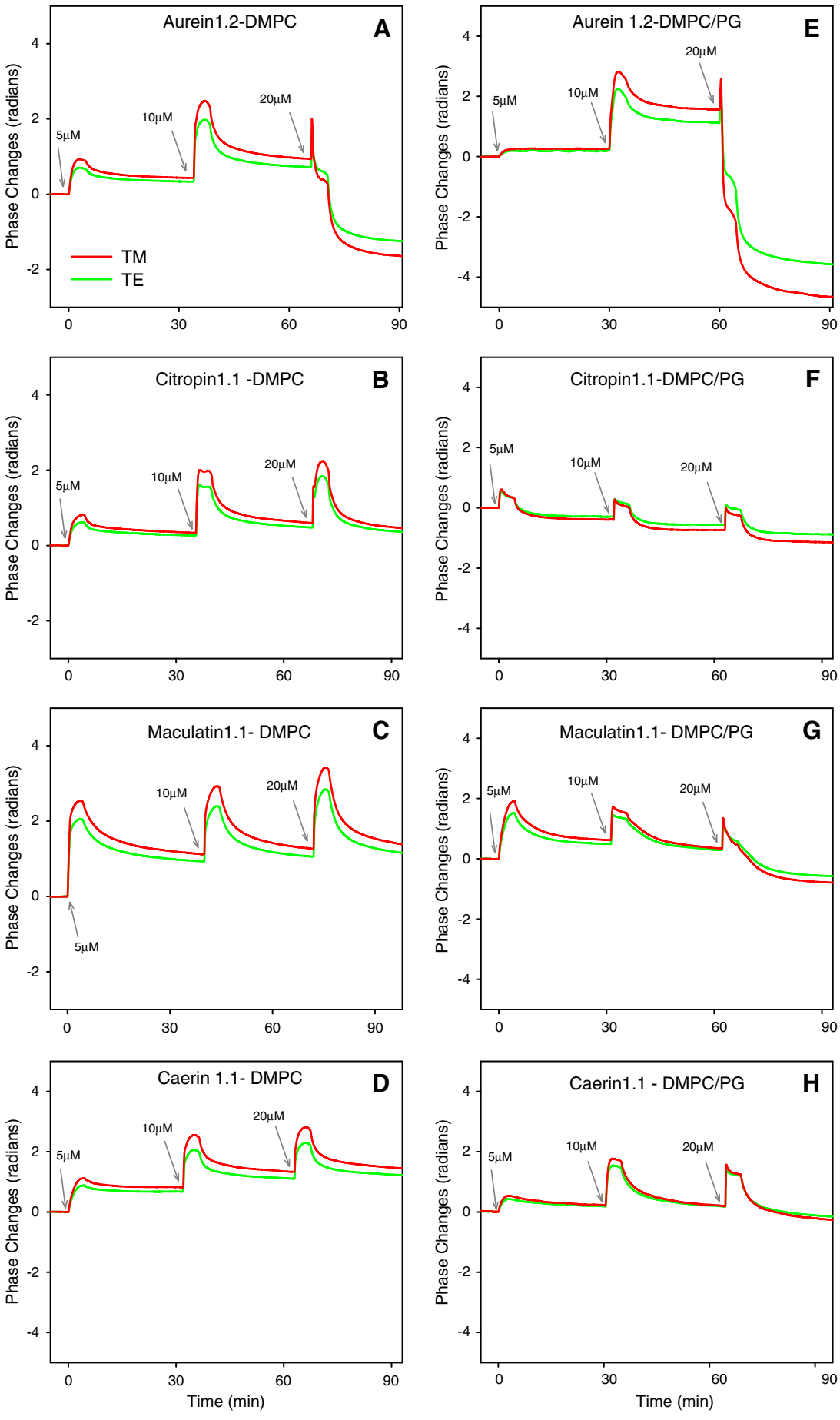
Aurein1.2-DMPC
A
Aurein 1.2-DMPC/PG
E
Citropin1.1 -DMPC
B
Citropin1.1-DMPC/PG
F
Maculatin1.1- DMPC
C
Maculatin1.1- DMPC/PG
G
Caerin 1.1- DMPC
D
Caerin1.1 - DMPC/PG
H
Phase Changes (radians)
Time (min)
5μM
10μM
20μM
TM
TE

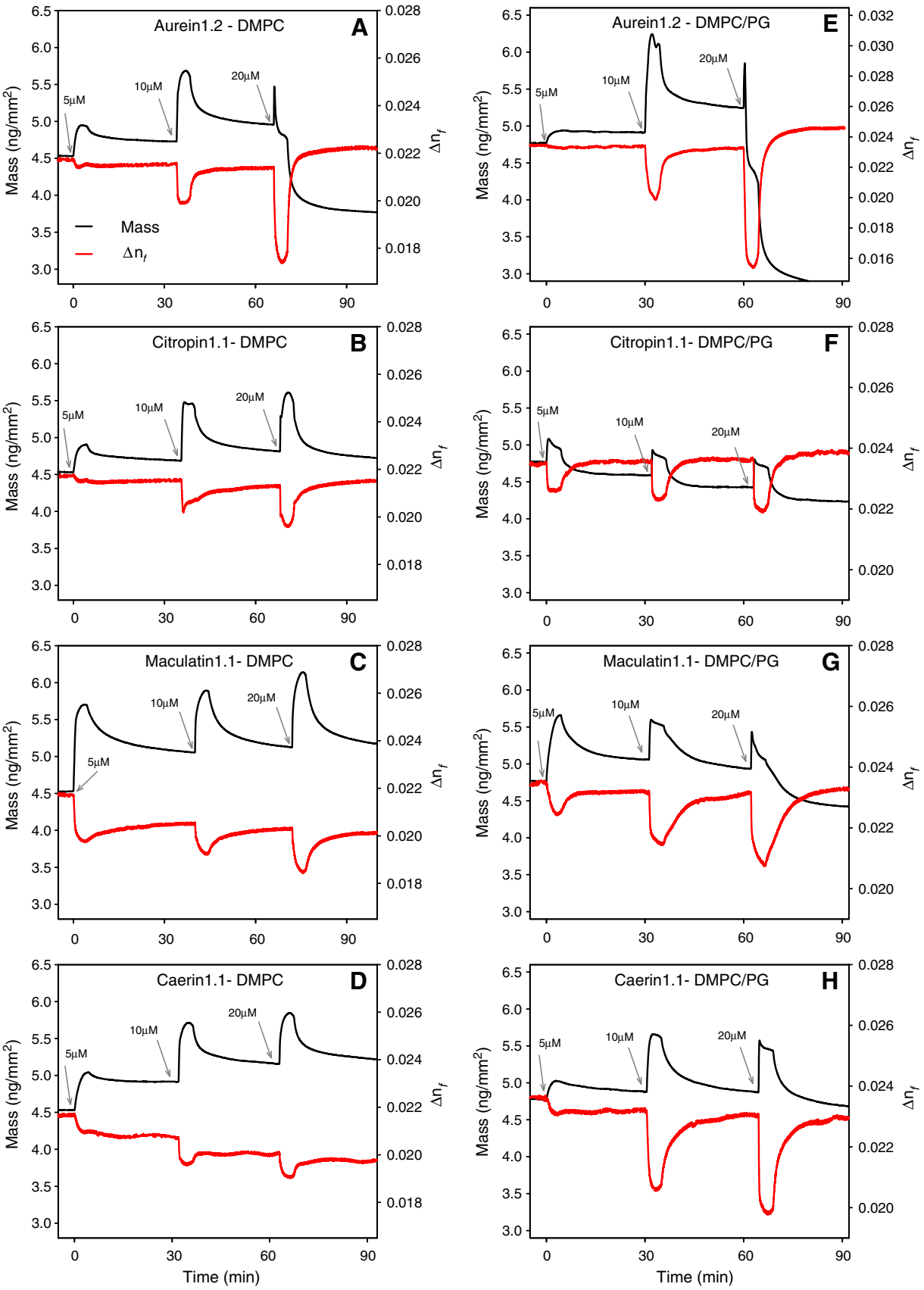

Fig. 3. The real time mass and birefringence changes for (A), (B) aurein 1.2; (C), (D) citropin 1.1; (E), (F) maculatin 1.1; and (G), (H) caerin 1.1; binding to a DMPC (A)–(D) or DMPC/DMPG (E)–(H) bilayer at 20 °C at 5 μM, 10 μM and 20 μM peptide. Mass is calculated by modelling the phase changes for both TM and TE modes using the assumed refractive index of DMPC, n = 1.4700.

Table 2
Maximum changes in mass bound and birefringence for DMPC and DMPC/DMPG bilayers for the initial binding of 5 μM of each peptide. Values were measured at the end of the association phase.

Bilayer parameters	Aurein 1.2	Citropin 1.1	Maculatin 1.1	Caerin 1.1
DMPC				
ΔMass (ng/mm^2)	0.310	0.278	0.867	0.379
ΔBirefringence	0.0000	−0.0002	−0.0019	−0.0008
DMPC/DMPG				
ΔMass (ng/mm^2)	0.411	0.263	0.408	0.188
ΔBirefringence	−0.0009	−0.0009	−0.0005	−0.0007

concentration. AFM analysis (Fig. S2) indicated that the DMPC vesicles upon addition of citropin 1.1 were fused and disintegrated into similar structures as seen for aurein 1.2, which disrupt model membranes via the carpet mechanism [26]. The DPI analysis also showed that citropin 1.1 bound less than aurein 1.1 to the DMPC bilayer.

The real time changes in bilayer mass for the binding of the longer peptides, maculatin 1.1 and caerin 1.1, to DMPC are shown in Fig. 3C and D, respectively. At 5 μM, maculatin 1.1 exhibited the strongest binding with fast association with the DMPC lipid layer with a maximum mass of 0.867 ng/mm^2 (Table 2) compared to the other three AMPs at this concentration. Maculatin 1.1 also showed a fast dissociation from the DMPC layer and gave the largest overall increase in mass, indicating a significant amount of peptide remained on the membrane after peptide dissociation. However, with consecutive injections of maculatin 1.1 at 10 and 20 μM, only a small increase in mass was noticed. This indicates that the saturation of maculatin1.1 for DMPC was reached and no further increase in mass was possible.

At 5 μM, caerin 1.1 associated strongly with the DMPC reaching a maximum mass of 0.319 ng/mm^2 at the end of injection (Table 2) with very little dissociation, resulting in an overall increase in the lipid layer of 0.286 ng/mm^2 in mass This amount is similar to that found for maculatin 1.1 at 5 μM. With consecutive injections of 10 μM and 20 μM, caerin 1.1 associated at a faster rate, with a very rapid initial increase followed by a slower increase to reach a maximum. There was also a small increase in the mass bound with each accumulative addition of caerin 1.1 to DMPC, similar to maculatin 1.1.

The mass changes for the binding of each peptide to the negatively charged DMPC/DMPG (4:1) bilayers are shown in Fig. 3E–H. At the lowest concentration of 5 μM, aurein 1.2 bound strongly to DMPC/DMPG with a maximum mass of 0.411 ng/mm^2 (Table 2), while at 10 μM, a small mass loss was observed during the association phase. In contrast to the DMPC bilayer, aurein 1.2 had the most significant effect in destabilising the lipid layer, with the biggest mass loss of 0.623 ng/mm^2 at 20 μM compared to the other peptides on the DMPC/DMPG bilayer, as previously reported [17]. This suggests that lysis of DMPC/DMPG membranes by aurein 1.2 is facilitated by a stronger and faster association mediated by the electrostatic interaction between the cationic group on the peptide and anionic lipid head group.

A smaller increase in mass was observed for the binding of 5 μM citropin 1.1 to the DMPC/DMPG bilayer with a maximum mass of 0.263 ng/mm^2 (Table 2). Similar to aurein 1.2, at higher concentrations citropin 1.1 rapidly bound and removed material from the DMPC/DMPG bilayer with a mass loss of 0.247 ng/mm^2 at 10 μM and 0.124 ng/mm^2 at 20 μM. These results are consistent with previous SPR analyses where some mass loss was observed for citropin 1.1 binding to the DMPC/DMPG membranes [16,17]. The results can also be correlated with the lysis of DMPC/DMPG bilayers evident by AFM (Fig. S2).

For maculatin 1.1, a high and fast association similar to that for DMPC was obtained with a significant amount of peptide strongly associated with the lipid layer with a maximum mass of 0.408 ng/mm^2 at the end of association and an overall mass increase of 0.185 ng/mm^2 at the end of the dissociation phase. At higher concentration, maculatin 1.1 appeared to remove material from the surface in a similar manner to aurein 1.2 and citropin 1.1. Comparison of the interaction of maculatin 1.1 with the two different lipid bilayers suggests that maculatin 1.1 has a preference for the anionic membrane with disruption of the DMPC/DMPG bilayer.

Unlike maculatin 1.1, caerin 1.1 showed a small and slow increase in mass during association with DMPC/DMPG at 5 μM with a minimal amount remaining bound to the bilayer. A faster and greater association for DMPC/DMPG was observed at 10 μM caerin concentration with a maximum mass of 0.868 ng/mm^2 at the end of association (Table 2). A small amount of material was removed after addition of 20 μM caerin 1.1. These results suggest that caerin is the least effective in membrane disruption.

3.3. Real time changes in bilayer birefringence during peptide binding

Analysis of changes in bilayer order (Δn_f) as a function of membrane-bound peptide mass (m_p) allows the impact of peptide binding in the membrane structure to be determined, whereby increases in Δn_f correspond to increased membrane order [17,27]. This allows the extent of membrane changes with peptide loading to be directly quantitated and the changes in DMPC and DMPC/DMPG bilayer order induced by each peptide are shown in Fig. 4.

For the interaction of 5 μM aurein 1.2 with DMPC (Fig. 4A) [17], birefringence remained at a constant value of 0.0220 throughout the whole process of association and dissociation (Table 2), which suggested that there was little or no membrane disordering, in contrast to the mass increases described above. For 10 μM aurein 1.2, the lipid molecules began to disorder as birefringence decreased to 0.0204. Furthermore, the curvature of the drop in birefringence indicated different kinetics in regard to the rate of disordering of the membrane during peptide association. Initially, birefringence decreased at a slower rate followed by a much steeper drop, which corresponds to a faster rate of membrane disordering with an increase in peptide on the surface. However, this disordering was temporary and lipid molecules reorganise and re-order during peptide dissociation as indicated by the return of the birefringence to the original value. At 20 μM, aurein 1.2 bound rapidly with significant disordering as birefringence decreased in a curved manner (similar to that observed at 10 μM) to 0.0200 before removal of material from the surface. The abrupt drop in mass coincided with a steeper drop in birefringence as the membrane destabilised at a peptide-to-lipid ratio (P/L*) of 1:14 (Table 3). At the end of peptide injection, the lipid and peptides continued to dissociate from the surface, while birefringence recovered to 0.0227. These combined results suggest that, during association, the membrane lysed with considerable disordering of the bilayer and loss of structure. Interestingly, during dissociation and following lysis, lipid molecules were able to rearrange with an increase in order. Reversal of birefringence back to the starting value after membrane lysis was also evident for the other peptides in this study.

The binding of citropin 1.1 at 5 μM to DMPC resulted in a minimal decrease in birefringence with a value of −0.0002 (Table 2) indicating that the peptide interacts with the membrane without changing the molecular order of the lipid matrix (Fig. 4B). As the concentration increased to 10 and 20 μM, additional peptide binding resulted in a decrease of birefringence during association but reverted back to the 5 μM values. The reversible changes in birefringence indicate that the DMPC molecular order and packing are transiently affected by citropin 1.1 binding and are consistent with surface binding.

The binding of maculatin 1.1 to DMPC showed a significant decrease in birefringence with a value of −0.0019 at the end of association for 5 μM and, unlike the curved drop for aurein1.2, the decrease was almost linear as for the mass change (Fig. 4C). In addition, birefringence did not recover, indicating significant change in the order and packing of the lipid bilayer. With cumulative injections of maculatin 1.1, at higher concentration, the change in birefringence was reversible with minimal

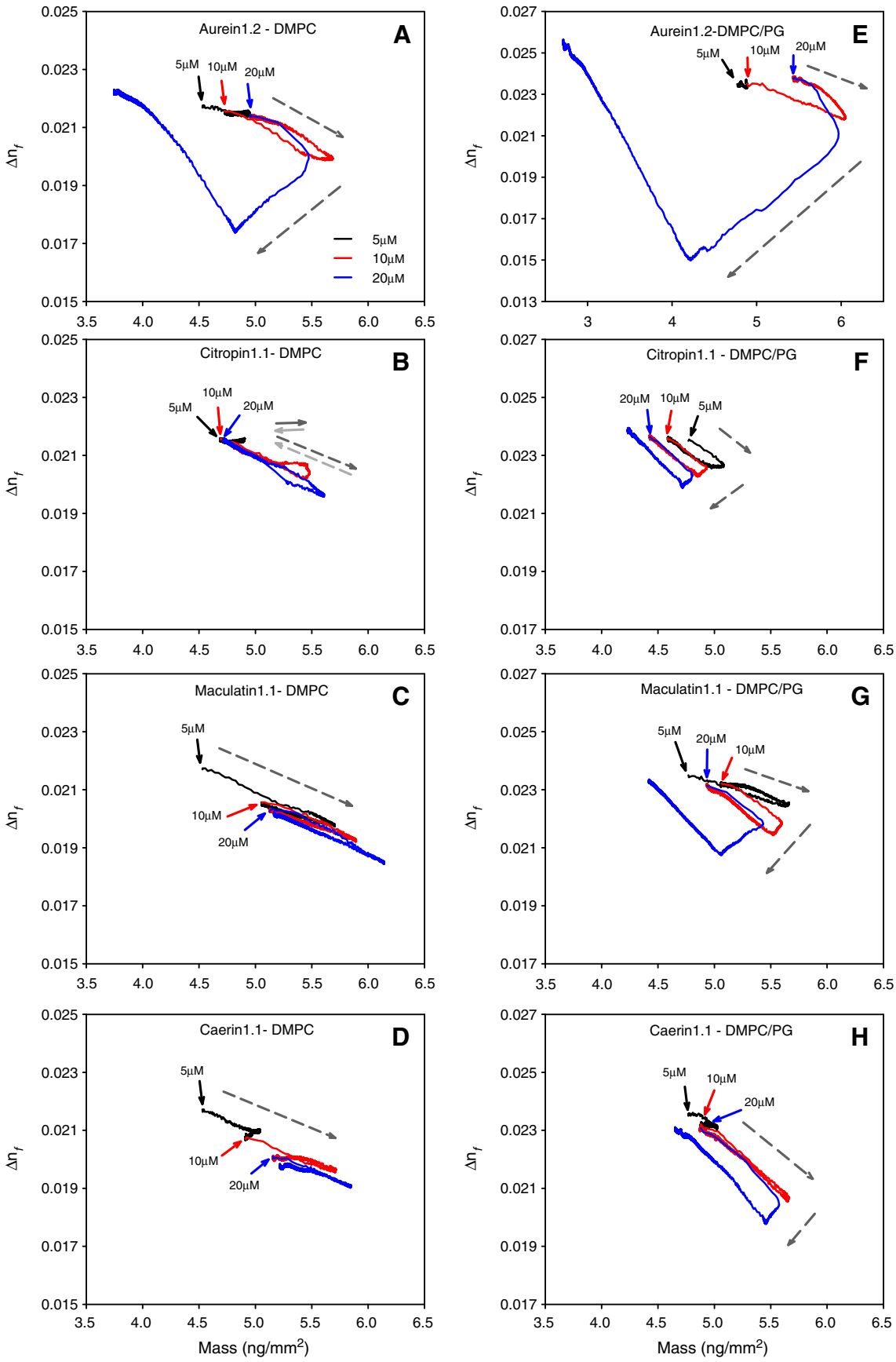

Fig. 4. The effect of: (A), (B) aurein 1.2; (C), (D) citropin 1.1; (E), (F) maculatin 1.1; and (G), (H) caerin 1.1; on the molecular order of a planar DMPC (A)–(D), or DMPC/DMPG (E)–(H) bilayer determined by the optical birefringence as a function of membrane-bound peptide mass.

Table 3
Peptide to lipid (P:L) ratio corresponding to a significant membrane destabilisation.

Peptide	DMPC	DMPC/DMPG (4:1)
Aurein 1.2	1:14 (10 μM)	1:23 (10 μM)
Citropin 1.1	-	1:31 (10 μM)
Maculatin 1.1	-	1:15 (10 μM)
Caerin 1.1	-	1:15 (20 μM)

'-' Coincident mass and birefringence drop not observed.

overall change after dissociation. Further addition of maculatin 1.1 had little effect on the DMPC order and packing.

For caerin 1.1 (Fig. 4D), similar to maculatin 1.1, birefringence decreased linearly with a value of −0.0008 as mass increased during DMPC association. The decrease in bilayer birefringence was not reversible at 5 μM and continued during peptide dissociation. With further addition of caerin 1.1 to DMPC, the decrease in birefringence returned to half point for 10 μM and was almost reversed for 20 μM. The change in birefringence and the increase in mass suggest that caerin 1.1 is able to incorporate into the DMPC bilayer and induce significant changes in lipid order and packing.

Aurein 1.2, citropin 1.1 and maculatin 1.1 binding to DMPC/DMPG bilayers showed similar decrease in birefringence (Fig. 4E–H). At 5 μM, aurein 1.2 and citropin 1.1 showed reversible changes in birefringence with a value of −0.0009 (Table 2), while maculatin1.1 induced a small irreversible decrease in birefringence (−0.0005, Table 2) with increase in mass. All three peptides resulted in mass loss for DMPC/DMPG bilayers at both 10 and 20 μM. It is worthy of note that, during the mass loss at 10 μM, no further decrease in birefringence was observed, while a further decrease in birefringence was seen together with mass loss during injection of 20 μM peptides. However, birefringence decreased in a curved manner for aurein 1.2, suggesting that peptide accumulation on the DMPC/DMPG surface increased the rate of disorder. Also, for both aurein 1.2 and citropin 1.1, the final birefringence of the destabilised DMPC/DMPG bilayer was higher than the original values. Thus, the lipid molecules are able to re-assemble in an ordered manner after membrane lysis and the bilayer becomes more anisotropic.

For caerin 1.1 binding to DMPC/DMPG (Fig. 4H), the low level of mass bound corresponded to very little change in birefringence with a value of −0.0007 at 5 μM (Table 2). In contrast, at higher concentrations caerin 1.1 induced a significant decrease in birefringence with a small mass loss at 20 μM. The decrease in birefringence was almost fully reversible on DMPC/DMPG which contrasts with the partial recovery of DMPC.

The plots of birefringence as a function of bound peptide mass for both lipid bilayers also reveal a critical concentration threshold at which a change in slope that corresponds to loss of mass can be determined. This value was expressed as a mass of bound peptide:lipid ratio (P/L*) for aurein 1.2 binding to DMPC and for each peptide binding to DMPC/DMPG bilayers and are listed in Table 3. These values range from 1:14 for aurein 1.2 on DMPC to 1:31 for citropin 1.1 on DMPC/DMPG and are consistent with P/L* obtained for fluorescence-dye leakage experiments [28].

4. Discussion

Antimicrobial activity for this family of amphibian peptides is dependent on membrane interaction in order to target and perturb cell function. For this reason, detailed information on the structure of the lipid membrane in the peptide–lipid interaction is essential to understanding the factors that control affinity and selectivity of AMPs for target cells. Furthermore, as AMPs are capable of exerting both antimicrobial and haemolytic effects, understanding the biophysical properties and mechanisms of action of these peptides against different membrane compositions is vital for the development of AMPs for therapeutic purposes.

Aurein 1.2, citropin 1.1, maculatin 1.1 and caerin 1.1 are a family of closely related AMPs whose physical properties can be correlated with their membrane-disruptive behaviour. It has been demonstrated, both in previous studies [8,13,14] and in the data presented here, that these peptides are unstructured in aqueous buffer but adopt substantial α-helical structure in the presence of DMPC and DMPC/DMPG liposomes. As a consequence, the resulting amphipathic structure is important for high affinity interactions with phospholipid bilayers. The amphipathicity decreases with increasing peptide length while the hydrophobicity increases in the order maculatin 1.1 < aurein 1.2 < citropin 1.1 < caerin 1.1. Previously we used DPI to investigate the effect of aurein 1.2 on membrane bilayer order and showed that this peptide exerts a dramatic effect on a range of phospholipid bilayers [17]. Moreover, aurein 1.2 caused significant lysis and removal of membrane from the surface with DMPC and DMPC/DMPG, but not on DMPC/DPMG/cholesterol, DMPE/DMPG or an *Escherichia coli* lipid mixture. Given the dramatic effects on DMPC and DMPC/DMPG, in the present study we have investigated and compared the effect of the four AMPs on DMPC and DMPC/DMPG.

Analysis of the birefringence plots (Fig. 4), together with the effect of the initial binding of each peptide on the bilayer (Table 2) and the P:L ratio at which the bilayer is disrupted (Table 3), provides a global overview of the effect of these peptides on bilayer integrity. At the lowest concentration (5 μM) on the neutral DMPC, the two shorter peptides (aurein 1.2 and citropin 1.1) bound a moderate amount and had very little effect on birefringence, suggesting surface binding at this concentration. At 10 μM, aurein 1.2 and citropin 1.1 binding increased substantially, and the birefringence also dropped, but subsequently recovered after peptide dissociation. Aurein 1.1 birefringence also showed a slight hysteresis (change in slope) during dissociation. Most dramatically, aurein 1.2 caused a large mass loss at 20 μM. In contrast, a high amount of maculatin 1.1 bound to the bilayer at the lowest concentration, causing a large drop in birefringence and only about half of the bound peptide dissociated allowing only partial recovery of birefringence. In comparison, caerin 1.1 (the longest peptide) bound a little more than aurein 1.2 and citropin 1.1, but caused a largely irreversible drop in birefringence. Maculatin 1.1 and caerin 1.1 both exhibited a reversible decline and recovery of birefringence at 10 μM and 20 μM. These results suggest that while aurein 1.2 destroys the DMPC bilayer, citropin 1.1 caused little damage, while the two longer peptides bound in a manner that caused a significant but partially reversible drop in bilayer order. By comparison, all peptides, except for maculatin 1.1, exerted more substantial effects on the anionic DMPC/DMPG bilayer. Aurein 1.2 exhibited a similar birefringence-mass profile, but there was even greater mass loss and disordering of the bilayer. Citropin 1.1, maculatin 1.1 and caerin 1.1 all caused a reversible drop in birefringence which was also associated with a moderate drop in mass, although the extent of change for maculatin 1.1 was less than observed on DPMC.

Aurein 1.2 has been proposed to act via a carpet-like mechanism while caerin 1.1 inserts into the bilayer to form pores [13]. While the description of this final state is useful to classify AMPs, the changes in the bilayer structure that occurs between initial peptide binding and this final lytic state provide a significant improvement in our understanding of AMP action. The transition from a detergent-like carpet mechanism to an insertion-pore-like mechanism in terms of bilayer disruption deduced from the birefringence-mass plots (Fig. 4) is depicted schematically in Fig. 5. Aurein 1.2 destroys bilayer structure and the birefringence-mass profiles for this peptide differ significantly from the profiles of the other three peptides which operate by a different mechanism after binding. Overall, three different transitions can be described based on the birefringence vs. mass plots, from which peptide behaviour or AMP mechanism may be deduced. These are (1) the aurein-like profile showing dramatic lysis and the two different citropin/maculatin/caerin-like profiles on either (2) DMPC or (3) DMPC/DMPG.

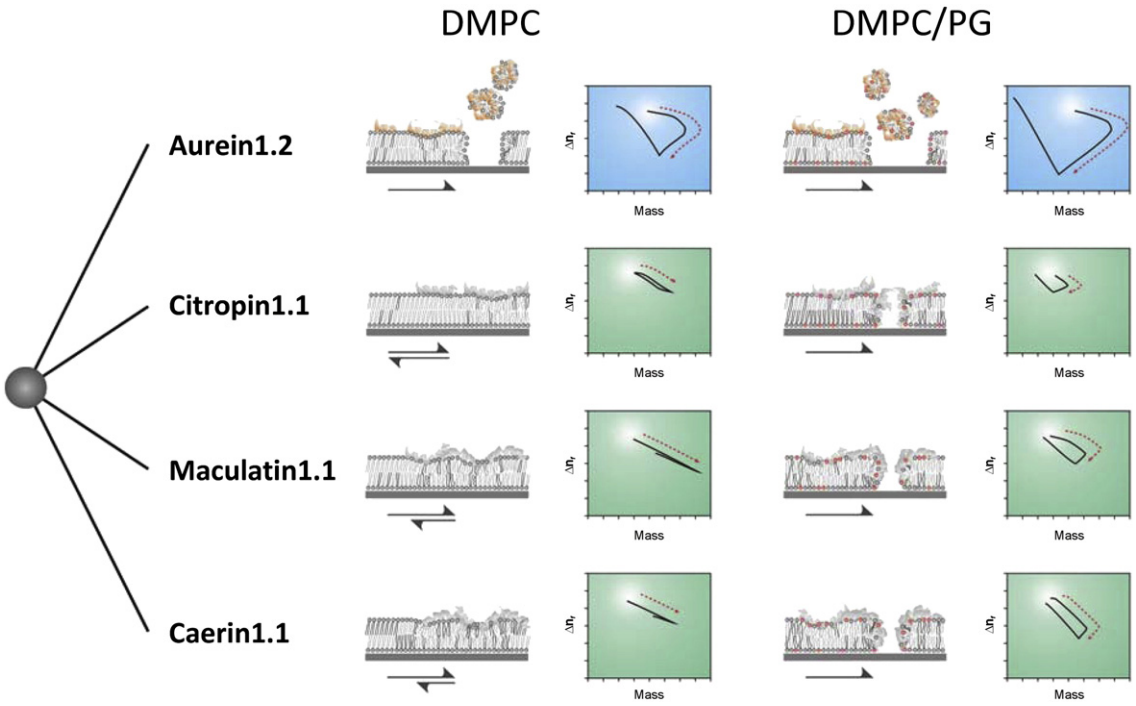

Fig. 5. Schematic depicting the different effects of each AMP on the structure of DMPC and DMPC/DMPG bilayers.

Since aurein 1.2 is unable to fully span a membrane, this short peptide acts in a detergent-like manner, facilitated by its highly amphipathic nature. Most significantly, pronounced bilayer disordering occurs at 10 μM prior to the lysis step evident at 20 μM, and the P:L ratios of 1:14 and 1:23 respectively demonstrates the critical level of surface binding is required to cause lysis [29].

As the peptide length increases, a change in mechanism is evident with the birefringence-mass profiles revealing a set of overlapping lines on DMPC. Citropin 1.1 caused much less disruption than aurein 1.2, demonstrating that the additional three amino acid residues diminish the ability of the peptide to "dissolve" the membrane in an aurein-like manner. After the irreversible decrease in birefringence for the binding of maculatin 1.1 and caerin 1.1 to DMPC, indicating relatively strong binding to the membrane, subsequent binding caused significant but reversible disordering of the acyl lipid chains with no substantial mass loss. However, the overlapping curves apparent on DMPC are in contrast to the rectangular plots of birefringence vs. mass on DMPC/DMPG suggesting a different mechanism of interaction and bilayer disturbance. The membrane disordering effect evident from the birefringence profiles for these peptides is also consistent with increased fluctuations in phospholipid bilayers observed by ^{31}P NMR relaxation times [16] and decrease in ^{2}H NMR order parameters [7,11,16,30]. These studies showed that surface-bound peptides disorder the bilayer more than peptides that insert, thereby increasing the area per head group, giving the chains a larger area to sample more angles and thus have a lower order parameter [7,11,16,30].

Taken together, the results demonstrate that maculatin 1.1 and caerin 1.1 bind strongly to DMPC and with increasing hydrophobicity are likely to penetrate somewhat and bind to the interfacial region of the bilayer. In contrast, in the presence of anionic DMPG, the charged peptides bind and insert into the bilayer to cause an apparent mass drop, but which is significantly less than observed for aurein 1.2. The extent of the drop in mass at each concentration can be associated with either loss of material from the surface or bilayer expansion for these longer peptides on the anionic bilayers as also confirmed by AFM (Fig. S2) and in a previous study [31]. Bilayer expansion has been recently shown to be a defined state in the interaction of the HPA peptide with DMPC [32,33] in which peptides insert and decrease the amount of bound material in the detection window, corresponding to the formation of pore-like structures in the bilayer. The series of rectangular plots evident for citropin 1.1, maculatin 1.1 and caerin 1.1 in Fig. 4 are, therefore, consistent with insertion and incremental expansion of the bilayer. Thus, as the peptides increase in length and hydrophobicity and decrease in amphipathicity, there is a transition from a surface-bound (aurein-like) to a more inserted state (maculatin/caerin-like), and this ability to insert is enhanced in DMPC/DMPG leading to expansion/pore formation. The differences in the degree of expansion evident for each peptide can also be related to their structures. Citropin 1.1 is the shortest of the three peptides (16 residues) but is the most similar to aurein 1.2 (13 residues), and caused disruption at the lowest surface loading of P:L = 1:31. Maculatin 1.1 contains 21 residues and contains a proline residue which has been shown to play a critical role in the disruption of the bilayer [12]. Finally, caerin 1.1 contains 25 residues, is the most hydrophobic of the four peptides and the critical P:L ratio of 1:15 was only reached at the highest concentration, reflecting a stronger surface binding prior to insertion into the bilayer.

Overall, the simultaneous measurement of the real-time changes in mass and molecular order as a result of AMP binding on lipid bilayers has provided a more detailed understanding of the mechanism of membrane disruption and lysis. While the process from initial peptide binding to the lipid bilayer and membrane destabilisation is complex, the multiple stages of membrane destabilisation can be deduced from the birefringence profiles. Moreover, the extent of peptide coverage on the membrane surface required for each membrane state can also be determined to differentiate and characterise the trigger point for membrane lysis. While the critical interplay between electrostatic and hydrophobic interactions is well established, this can now be rationalised in terms of bilayer structural changes and DPI can be used to differentiate the binding mechanism of closely related cationic AMPs. In particular, the lytic activity of these peptides is likely to be mediated by significant changes in the membrane structure which has not been previously demonstrated. More direct correlations between the antibacterial data and the membrane-disruptive properties shown

in this study will be possible when birefringence measurements of bacterial membrane extracts are performed.

Acknowledgements

The financial support of the Australian Research Council and the Heart Foundation of Australia is gratefully acknowledged.

Appendix A. Supplementary data

Supplementary data to this article can be found online at http://dx.doi.org/10.1016/j.bbamem.2014.02.017.

References

[1] C. Arias, B. Murray, Antibiotic-resistant bugs in the 21st century — a clinical super-challenge, N. Engl. J. Med. 360 (2009) 439–443.
[2] E. Klein, D. Smith, R. Laxminarayan, Hospitalizations and deaths caused by methicillin-resistant *Staphylococcus aureus*, United States, 1999–2005, Emerg. Infect. Dis. 13 (2007) 1840–1846.
[3] R. Moellering, Discovering new antimicrobial agents, Int. J. Antimicrob. Agents 37 (2011) 2–9.
[4] R.E. Hancock, H.G. Sahl, Antimicrobial and host-defense peptides as new anti-infective therapeutic strategies, Nat. Biotechnol. 24 (2006) 1551–1557.
[5] T. Rozek, K.L. Wegener, J.H. Bowie, I.N. Olver, J.A. Carver, J.C. Wallace, M.J. Tyler, The antibiotic and anticancer active aurein peptides from the Australian Bell Frogs Litoria aurea and Litoria raniformis the solution structure of aurein 1.2, Eur. J. Biochem. 267 (2000) 5330–5341.
[6] M.A. Apponyi, T.L. Pukala, C.S. Brinkworth, V.M. Maselli, J.H. Bowie, M.J. Tyler, G.W. Booker, J.C. Wallace, J.A. Carver, F. Separovic, J. Doyle, L.E. Llewellyn, Host-defence peptides of Australian anurans: structure, mechanism of action and evolutionary significance, Peptides 25 (2004) 1035–1054.
[7] D.I. Fernandez, J.D. Gehman, F. Separovic, Membrane interactions of antimicrobial peptides from Australian frogs, Biochim. Biophys. Acta 1788 (2009) 1630–1638.
[8] M.S. Balla, J.H. Bowie, F. Separovic, Solid-state NMR study of antimicrobial peptides from Australian frogs in phospholipid membranes, Eur. Biophys. J. 33 (2004) 109–116.
[9] D.I. Fernandez, A.P. Le Brun, T.H. Lee, P. Bansal, M.I. Aguilar, M. James, F. Separovic, Structural effects of the antimicrobial peptide maculatin 1.1 on supported lipid bilayers, Eur. Biophys. J. 42 (2013) 47–59.
[10] E.E. Ambroggio, F. Separovic, J. Bowie, G.D. Fidelio, Surface behaviour and peptide-lipid interactions of the antibiotic peptides, Maculatin and Citropin, Biochim. Biophys. Acta 1664 (2004) 31–37.
[11] D.I. Fernandez, M.A. Sani, F. Separovic, Interactions of the antimicrobial peptide maculatin 1.1 and analogues with phospholipid bilayers, Aust. J. Chem. 64 (2011) 798–805.
[12] D.I. Fernandez, T.H. Lee, M.A. Sani, M.I. Aguilar, F. Separovic, Proline facilitates membrane insertion of the antimicrobial peptide maculatin 1.1 via surface indentation and subsequent lipid disordering, Biophys. J. 104 (2013) 1495–1507.
[13] D.I. Fernandez, M.A. Sani, A.J. Miles, B.A. Wallace, F. Separovic, Membrane defects enhance the interaction of antimicrobial peptides, aurein 1.2 versus caerin 1.1, Biochim. Biophys. Acta 1828 (2013) (1863–1872).
[14] J.H. Bowie, F. Separovic, M.J. Tyler, Host-defense peptides of Australian anurans. Part 2. Structure, activity, mechanism of action, and evolutionary significance, Peptides 37 (2012) 174–188.
[15] W.C. Wimley, K. Hristova, Antimicrobial peptides: successes, challenges and unanswered questions, J. Membr. Biol. 239 (2011) 27–34.
[16] J.D. Gehman, F. Luc, K. Hall, T.-H. Lee, M.P. Boland, T.L. Pukala, J.H. Bowie, M.I. Aguilar, F. Separovic, Effect of antimicrobial peptides from Australian tree frogs on anionic phospholipid membranes, Biochemistry 47 (2008) 8557–8565.
[17] T.-H. Lee, C. Heng, M. Swann, J. Gehman, F. Separovic, M. Aguilar, Real-time quantitative analysis of lipid disordering by aurein 1.2 during membrane adsorption, destabilisation and lysis, Biochim. Biophys. Acta, Biomembr. (2010) 1977–1986.
[18] A. Mashaghi, M. Swann, J.P.M. Textor, E. Reimhult, Optical anisotropy of supported lipid structures probed by waveguide spectroscopy and its application to study of supported lipid bilayer formation kinetics, Anal. Chem. 80 (2008) 3666–3676.
[19] J. Popplewell, N. Freeman, S. Carrington, G. Ronan, C. McDonnell, R.C. Ford, Quantification of the effects of melittin on liposome structure, Biochem. Soc. Trans. 33 (2005) 931–933.
[20] C.J. Terry, J.F. Popplewell, M.J. Swann, N.J. Freeman, D.G. Fernig, Characterisation of membrane mimetics on a dual polarisation interferometer, Biosens. Bioelectron. 22 (2006) 627–632.
[21] J.L. Fauchere, V. Pliska, Hydrophobic parameters {pi} of amino-acid side chains from the partitioning of N-acetyl-amino-acid amides, Eur. J. Med. Chem. 8 (1983) 369–375.
[22] R. Gautier, D. Douguet, B. Antonny, G. Drin, HELIQUEST: a web server to screen sequences with specific α-helical properties, Bioinformatics 24 (2008) 2101–2102.
[23] T. Rozek, J.H. Bowie, J.C. Wallace, M.J. Tyler, The antibiotic and anticancer active aurein peptides from the Australian Bell Frogs Litoria aurea and Litoria raniformis. Part 2. Sequence determination using electrospray mass spectrometry, Rapid Commun. Mass Spectrom. 14 (2000) (2002–2011).
[24] T. Rozek, R.J. Waugh, S.T. Steinborner, J.H. Bowie, M.J. Tyler, J.C. Wallace, The maculatin peptides from the skin glands of the tree frog Litoria genimaculata: a comparison of the structures and antibacterial activities of maculatin 1.1 and caerin 1.1, J. Pept. Sci. 4 (1998) 111–115.
[25] K.L. Wegener, P.A. Wabnitz, J.A. Carver, J.H. Bowie, B.C. Chia, J.C. Wallace, M.J. Tyler, Host defence peptides from the skin glands of the Australian blue mountains tree-frog Litoria citropa. Solution structure of the antibacterial peptide citropin 1.1, Eur. J. Biochem. 265 (1999) 627–637.
[26] D.I. Fernandez, A.P. Le Brun, T.C. Whitwell, M.A. Sani, M. James, F. Separovic, The antimicrobial peptide aurein 1.2 disrupts model membranes via the carpet mechanism, Phys. Chem. Chem. Phys. 14 (2012) 15739–15751.
[27] T.-H. Lee, K. Hall, M. Swann, J. Popplewell, S. Unabia, Y. Park, K. Hahm, M. Aguilar, The membrane insertion of helical antimicrobial peptides from the N-terminus of *Helicobacter pylori* ribosomal protein L1, Biochim. Biophys. Acta, Biomembr. (2010) 544–557.
[28] E.E. Ambroggio, F. Separovic, J.H. Bowie, G.D. Fidelio, L.A. Bagatolli, Direct visualization of membrane leakage induced by the antibiotic peptides: maculatin, citropin, and aurein, Biophys. J. 89 (2005) 1874–1881.
[29] M.N. Melo, R. Ferre, M.A. Castanho, Antimicrobial peptides: linking partition, activity and high membrane-bound concentrations, Nat. Rev. Microbiol. 7 (2009) 245–250.
[30] D.I. Fernandez, M.A. Sani, J.D. Gehman, K.S. Hahm, F. Separovic, Interactions of a synthetic Leu-Lys-rich antimicrobial peptide with phospholipid bilayers, Eur. Biophys. J. 40 (2011) 471–480.
[31] A. Mechler, S. Praporski, K. Atmuri, M. Boland, F. Separovic, L.L. Martin, Specific and selective peptide-membrane interactions revealed using quartz crystal microbalance, Biophys. J. 93 (2007) 3907–3916.
[32] D.J. Hirst, T.H. Lee, M.J. Swann, M.I. Aguilar, Combined mass and structural kinetic analysis of multistate antimicrobial peptide–membrane interactions, Anal. Chem. 85 (2013) 9296–9304.
[33] D.J. Hirst, T.H. Lee, M.J. Swann, S. Unabia, Y. Park, K.S. Hahm, M.I. Aguilar, Effect of acyl chain structure and bilayer phase state on binding and penetration of a supported lipid bilayer by HPA3, Eur. Biophys. J. 40 (2011) 503–514.